

Quantum Density Estimation with Density Matrices in NISQ Devices: Application to Quantum Anomaly Detection

Diego H. Useche,* Oscar A. Bustos-Brinez, Joseph A. Gallego, and Fabio A. González†
MindLab Research Group, Universidad Nacional de Colombia, Bogotá, Colombia

(Dated: February 21, 2023)

Density estimation is a central task in statistics and machine learning. This problem consists of determining the underlying probability distribution that fits an observed data set. Despite its relevance, few works have explored quantum algorithms for density estimation. In this article, we present a novel classical-quantum density estimation model based on the expected values of density matrices and a new quantum variational kernel learning strategy. The method uses quantum hardware to encode probability distributions of training data via mixed quantum states. As a core subroutine, we present a new method to estimate the expected value of a mixed density matrix based on its spectral decomposition on a quantum computer. In addition, we illustrate an application of the method for classical-quantum anomaly detection. The density estimation model is tested with both quantum random and adaptive Fourier features on various data sets; results show the superior performance of quantum adaptive Fourier features for density estimation and anomaly detection. An important finding of this work is to show that it is possible to perform density estimation and anomaly detection with high performance on noise intermediate-scale quantum computers.

I. INTRODUCTION

Density estimation (DE) is an important problem in machine learning and statistics, which consists of determining the probability density function $p(\mathbf{x})$ from a set of samples drawn from an unknown probability distribution. Some applications of density estimation in machine learning include clustering [1, 2], anomaly detection [3, 4], and generative modeling [5]. Many classical algorithms have been proposed for DE [6–9]; however, there are only a handful of works that address the problem on quantum devices [10–13], of which some illustrate computational advantage [13].

In this article, we present a novel classical-quantum density estimation strategy for current noisy quantum computers, which combines quantum algorithms to compute the expectation values of density matrices with a new quantum variational representation of data called quantum adaptive Fourier features (QAFF). The proposed method builds probability distributions of data in the form of mixed quantum states in quantum hardware. The DE proposal is based on the DMKDE algorithm [14], which was originally developed as a quantum-inspired method for density estimation that efficiently approximates [15] kernel density estimation (KDE) [6, 7]; it fuses density matrices with random Fourier features (RFF) [16] to build a non-parametric density estimator.

As one of the main results, we present two protocols to estimate the expected value of a mixed density matrix in a quantum computer, through quantum circuits used to implement the DMKDE. In contrast to methods like quantum state tomography [17], which codify a density matrix in terms of the Pauli matrices, the proposed pro-

ocols codify a density matrix from its spectral decomposition and as a mixture of non-necessarily orthogonal pure states. In addition, we propose the quantum adaptive Fourier features (QAFF), a new quantum variational feature strategy suitable to both classical and quantum computers, which trains quantum maps in the Fourier basis [18] with a quantum strategy based on adaptive Fourier features (AFF) [16, 19]. It represents classical data as quantum states, where the squared inner product in the Hilbert space approximates a Gaussian kernel in the original space. We show that QAFF in conjunction with the DMKDE quantum algorithm allows us to perform quantum density estimation (QDE) with a reduced number of components in both a quantum simulator and a real noisy quantum computer. Furthermore, we present a quantum anomaly detection (QAD) strategy based on the proposed QDE method. We show that it is possible to perform both quantum density estimation and anomaly detection on noise intermediate-scale quantum (NISQ) devices [20]. In sum, the contributions of the article are as follows:

- (i) A new quantum variational feature mapping approach referred to as QAFF, which can be viewed as an adaptive version of random Fourier features [16].
- (ii) Two innovative quantum algorithms for estimating the expected value of a density matrix through its eigendecomposition or as a mixture of non-orthogonal pure states.
- (iii) A hybrid classical-quantum density estimation method for NISQ computers that combines Fourier features and quantum algorithms for expected value estimation.
- (iv) A classical-quantum anomaly detection strategy built on the proposed quantum density estimation approach.

* diusecher@unal.edu.co

† fagonzalez@unal.edu.co

The outline of the document is as follows: in Sect. II, we describe the related work, in Sect. III, we present the theoretical background of the DMKDE algorithm and the notation for the description of the quantum circuits, in Sect. IV, we introduce our proposed quantum density estimation method, outline the proposed quantum circuits to estimate the expected value of a mixed state density matrix, and show the proposed quantum adaptive Fourier features, in Sect. V, we illustrate the results of our proposed method for density estimation, in Sect. VI we illustrate the application of the method for quantum anomaly detection and in Sect. VII, we establish our conclusions and future outlook.

II. RELATED WORK

Density estimation is an important challenge for classical and quantum machine learning. The two main approaches of DE are parametric and non-parametric techniques. Parametric density estimation (PDE) aims to adjust the observed data to a prior probability distribution $p(\mathbf{x}, \theta)$, for instance, it may search for the parameters θ that fit the data with a Gaussian distribution. By contrast, non-parametric density estimation (NPDE) does not assume a particular form of the density function. Both PDE and NPDE methods have been widely addressed in classical computers [6–9, 21, 22]. Some early works of quantum density estimation build parametric models based on multivariate Gaussian distributions on quantum devices [10, 13]. Furthermore, the DMKDE [14] is a NPDE method that was initially developed for classical computers. However, the method can be implemented in quantum computers with both pure and mixed states; the pure state approach was developed in qubit-based quantum computers [12], while the mixed state version was implemented in a high-dimensional quantum computer [11]. In this article, we present a quantum algorithm to estimate the expected value of a density matrix that extends the mixed state DMKDE to qubits for NPDE in NISQ computers.

Other quantum machine learning models based on mixed states, include quantum support vector machines [23] and other kernel-based methods [24–27]. These models require the preparation of mixed quantum states in a quantum computer through purification [23, 28], or by a classical sampling of pure quantum states [24, 27]. In addition, it is possible to codify a density matrix in the Pauli basis, like in the variational quantum eigensolver [29], and quantum state tomography [17, 30–32], and using the density matrix exponentiation method [33], which encodes an exponential form of the density matrix by a unitary transformation, in analogy with the hamiltonian as the generator of time evolution. Our method departs from the aforementioned techniques, by encoding a density matrix for expected value estimation from its spectral decomposition and as a mixture of non-necessarily orthogonal pure states.

González et. al. [34] proposed the use of random Fourier features (RFF) [16] as quantum feature maps. RFF approximates shift-invariant kernels by calculating an explicit mapping to a low-dimensional feature space. Enhancing the power of random Fourier features to approximate shift-invariant kernels is an active area of research in classical computers. Two of the main approaches to the problem include refining the original RFF Monte Carlo sampling [35–37] and using optimization techniques to find the optimal Fourier parameters [38, 39]. Among the techniques based on optimization, adaptive Fourier features (AFF) [19] uses a siamese neural network to look for the optimal Fourier weights which reduce the mean squared distance between the Gaussian kernel and its Fourier feature approximation.

In this document, we present quantum adaptive Fourier features (QAFF), a quantum variational method analogous to AFF, which induces a Gaussian kernel between classical data samples in quantum devices, with a reduced number of components. Previous works [18, 40] have shown that quantum Fourier mappings can be used to build models which are universal function approximators. In addition, it is also possible to use coherent states as quantum maps to induce Gaussian kernels [41]. The proposed method learns the frequencies of the quantum Fourier maps with a quantum adaptive Fourier strategy.

III. PRELIMINARIES

In this section, we present the density matrix kernel density estimation algorithm (DMKDE) proposed by Gonzalez et al. [14], which is an efficient approximation of the Parzen–Rosenblatt window [6, 7]; the DMKDE method combines density matrices and random Fourier features [16] to estimate probability density functions from data.

A. Kernel Density Estimation

Kernel density estimation, also called the Parzen–Rosenblatt window [6, 7], is a non-parametric method for density estimation. Given a training data set, $\{\mathbf{x}_j\} \in \mathbb{R}^D$ and a kernel, the method builds a density estimator of a new test sample $\mathbf{x}^* \in \mathbb{R}^D$ by computing the kernel between all elements in the training data set and the test sample $k(\mathbf{x}_j, \mathbf{x}^*) = e^{-\gamma \|\mathbf{x}_j - \mathbf{x}^*\|^2}$, where γ (gamma) is termed the bandwidth, here we consider the Gaussian kernel. The probability density of the test sample \mathbf{x}^* is given by,

$$p_\gamma(\mathbf{x}^*) = \frac{1}{NM_\gamma} \sum_{j=1}^N k(\mathbf{x}_j, \mathbf{x}^*) = \frac{1}{NM_\gamma} \sum_{j=1}^N e^{-\gamma \|\mathbf{x}_j - \mathbf{x}^*\|^2}, \quad (1)$$

where, $M_\gamma = (\pi/\gamma)^{\frac{D}{2}}$. This method scales with the size of the training data set.

B. Density Matrix Kernel Density Estimation and Random Fourier Features

The machine learning algorithm density matrix kernel density estimation (DMKDE) [14] is a non-parametric method for density estimation that does not require optimization and works as an efficient approximation of kernel density estimation [6, 7].

The DMKDE method starts by applying a quantum feature map, based on quantum random Fourier features (QRFF) [16, 34], to each sample in the train and test data set $\{\mathbf{x}_j\} \rightarrow \{|\psi(\mathbf{x}_j)\rangle\}$, where $\mathbf{x}_j \in \mathbb{R}^D$ and $|\psi(\mathbf{x}_j)\rangle \in \mathbb{C}^d$ with $\langle\psi(\mathbf{x}_j)|\psi(\mathbf{x}_j)\rangle = 1$. The QRFF quantum technique creates a quantum embedding whose squared inner product approximates a shift-invariant positive definite kernel $|\langle\psi(\mathbf{x})|\psi(\mathbf{y})\rangle|^2 \approx k(\mathbf{x}, \mathbf{y})$, see Sect. IV A; in this article we use the Gaussian kernel $k(\mathbf{x} - \mathbf{y}) = e^{-\gamma\|\mathbf{x}-\mathbf{y}\|^2}$. The parameters of the QRFF are the inverse of the variance of the Gaussian kernel, denoted by γ (gamma), and the dimension of the quantum features d .

Once the random Fourier feature map is established, the DMKDE method builds a training density matrix. For the training states $|\psi(\mathbf{x}_j)\rangle$ for $j \in \{1, \dots, N\}$, the training mixed state is constructed by,

$$\rho_{\text{train}} = \frac{1}{N} \sum_{j=1}^N |\psi(\mathbf{x}_j)\rangle \langle\psi(\mathbf{x}_j)|, \quad (2)$$

The probability density estimator of a testing sample $\mathbf{x}^* \rightarrow |\psi(\mathbf{x}^*)\rangle$ is computed by,

$$\hat{p}_\gamma(\mathbf{x}^*) = \frac{1}{M_\gamma} \langle\psi(\mathbf{x}^*)| \rho_{\text{train}} |\psi(\mathbf{x}^*)\rangle. \quad (3)$$

The complexity of the prediction phase of the DMKDE algorithm is $O(d^2)$, which is independent of the size of the training data. Furthermore, by replacing Eq. 2 on Eq. 3, we obtain,

$$\begin{aligned} \hat{p}_\gamma(\mathbf{x}^*) &= \frac{1}{M_\gamma} \langle\psi(\mathbf{x}^*)| \left(\frac{1}{N} \sum_{j=1}^N |\psi(\mathbf{x}_j)\rangle \langle\psi(\mathbf{x}_j)| \right) |\psi(\mathbf{x}^*)\rangle \\ &= \frac{1}{NM_\gamma} \sum_{j=1}^N |\langle\psi(\mathbf{x}_j)|\psi(\mathbf{x}^*)\rangle|^2 \\ &\approx \frac{1}{NM_\gamma} \sum_{j=1}^N e^{-\gamma\|\mathbf{x}_j-\mathbf{x}^*\|^2}. \end{aligned}$$

Hence, the DMKDE algorithm in conjunction with QRFF is an efficient approximation of the Parzen–Rosenblatt window [6, 7]. In this document, we consider the DMKDE with QRFF [14] as a baseline for the proposed classical-quantum implementation of the DMKDE with quantum adaptive Fourier features (discussed in Sect. IV A).

C. Notation for the quantum circuits

We now introduce the notation of the quantum circuits used in the article, which is the same notation used in Ref. [42]. Any state of the canonical basis of an n -qubit state can be written as $|b_0b_1 \dots b_{n-1}\rangle$ with $b_i \in \{0, 1\}$, hence, we may write any state in the canonical basis as a string in its binary form. This notation can be simplified by writing such state as $|\sum_{i=0}^{n-1} b_i 2^i\rangle_n$, namely, the bit-string is written in decimal form and the subindex indicates the number of qubits of the state. For example, the 4-qubit state $|1010\rangle$ can be written as $|5\rangle_4$. We make use of the same subindex to illustrate the number of qubits that build a unitary gate or a quantum state.

IV. QUANTUM DENSITY ESTIMATION METHOD

We propose a hybrid classical-quantum model for density estimation based on the DMKDE algorithm [14] and the novel quantum adaptive Fourier features. Fig. 1 shows the main steps of the method: (i) quantum feature map, (ii) training phase, and (iii) density estimation of new samples. Step (i) is a hybrid classical-quantum variational algorithm, the step (ii) is calculated in a classical computer, while step (iii) is computed in a quantum computer. These steps are explained in more detail below.

- (i) Quantum feature map: Apply a feature map $\{\mathbf{x}_j\} \rightarrow \{|\psi(\mathbf{x}_j)\rangle\}$, based on QAFF, see Sect. IV A, to both train and test partitions; the training data corresponds to the classical data whose probability density we wish to estimate, while the test data corresponds to a grid of points in the same euclidean classical space of the training data. As a baseline, we also apply a quantum map based on quantum random Fourier features [16, 34].
- (ii) Training phase: Use a classical computer to build the training density matrix ρ_{train} from the training features, see Eq. 2, and calculate its spectral decomposition, $\rho_{\text{train}} = V\Lambda V^\dagger$. The training mixed quantum state encodes a probability distribution of the training dataset.
- (iii) Prediction phase: Estimate the probability density values of the test partition by computing the probability estimation of the test samples with the training density matrix. To calculate the probability estimator, see Eq. 3, use the proposed quantum circuit shown in Fig. 3. See Sect. IV B for the mathematical details of the DMKDE quantum circuit.

In the next sections, we present the theoretical details of the new quantum adaptive Fourier features method, and the proposed DMKDE quantum protocol to compute

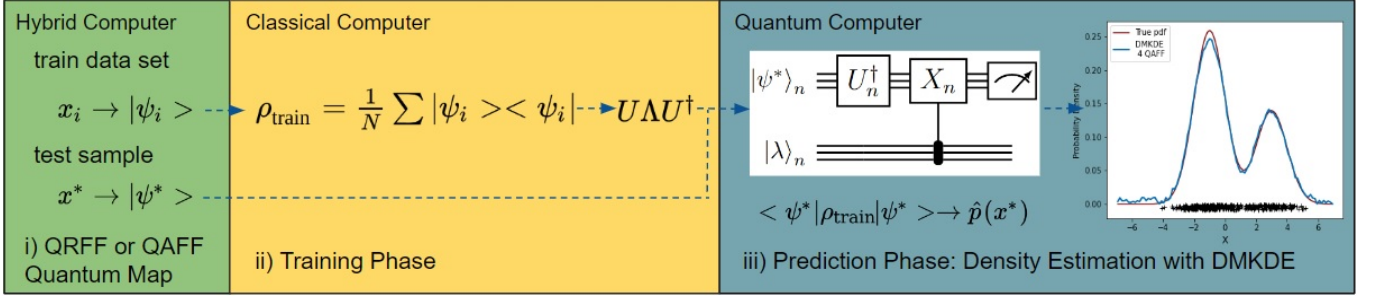


FIG. 1. Classical-quantum density estimation model for NISQ devices. It is also possible to perform the training phase in quantum hardware by the non-NISQ algorithm presented in App. B.

the expected value of a spectrally-decomposed mixed density matrix.

A. Quantum Adaptive Fourier Features

To build the quantum features of the quantum density estimation method, we propose the quantum adaptive Fourier features (QAFF), see Fig. 2; a novel quantum variational strategy that combines quantum Fourier maps [18, 40] with adaptive Fourier features [16, 19]. The QAFF method builds a quantum variational embedding which approximates a Gaussian kernel $k(\mathbf{x}, \mathbf{y}) = e^{-\gamma\|\mathbf{x}-\mathbf{y}\|^2}$, by mapping classical data samples $\mathbf{x} \in \mathbb{R}^D$ to quantum state-like representations $|\psi(\mathbf{x})\rangle \in \mathbb{C}^d$, such that, $\hat{k}_{\{\mathbf{w}_j\}}(\mathbf{x}, \mathbf{y}) = |\langle\psi(\mathbf{x})|\psi(\mathbf{y})\rangle|^2$ is an estimator of $k(\mathbf{x}, \mathbf{y})$. The method uses a quantum variational circuit to find the optimal parameters $\{\mathbf{w}_j\} \in \mathbb{R}^D$,

$$|\psi(\mathbf{x})\rangle = \sqrt{\frac{1}{d}} [e^{i\sqrt{\gamma}\mathbf{w}_0 \cdot \mathbf{x}}, e^{i\sqrt{\gamma}\mathbf{w}_1 \cdot \mathbf{x}}, \dots, e^{i\sqrt{\gamma}\mathbf{w}_{d-1} \cdot \mathbf{x}}]' \quad (4)$$

which minimize the loss function,

$$\mathcal{L}_{\{\mathbf{w}_j\}} = \frac{1}{N^2} \sum_{l=1}^N \sum_{m=1}^N (k(\mathbf{x}_l, \mathbf{x}_m) - \hat{k}_{\{\mathbf{w}_j\}}(\mathbf{x}_l, \mathbf{x}_m))^2. \quad (5)$$

An optimization-free strategy is possible by sampling the weights $\{\mathbf{w}_j\}$, of Eq. 4, from $\mathcal{N}(\mathbf{0}, \mathbf{I})$, this strategy corresponds to quantum random Fourier features (QRFF), which is also an estimator of the Gaussian kernel [16].

Since the loss function involves computing the kernel classically of every pair of data points, it is sufficient to use only a subset of training points for learning the kernel. In addition, considering that the Gaussian kernel is shift-invariant, we may also train the kernel with a synthetic data set, which corresponds to sampled points whose pair-wise euclidean distance is of the same order of magnitude as the width σ of the Gaussian kernel; for instance, we may take points between $[-10\sigma, 10\sigma]$ to learn the one-dimensional kernel $e^{-(x-y)^2/2\sigma^2}$.

Also, we may ignore the global phase by setting $\mathbf{w}_0 = \mathbf{0}$, this reduces the algorithm to $(d-1)D$ quantum variational parameters.

1. Quantum variational implementation of QAFF

The proposed QAFF method can be trained classically using neural networks [19, 45]. Here, we present a quantum variational strategy for QAFF, see Fig. 2.

To prepare the quantum state $|\psi(\mathbf{x})\rangle$, see Eq. 4, we first show the case of one-dimensional data. In this case the quantum state corresponds to $|\psi(x)\rangle = \sqrt{\frac{1}{d}} [1, e^{i\sqrt{\gamma}w_1x}, \dots, e^{i\sqrt{\gamma}w_{d-1}x}]'$. We may prepare this state with $n = \log d$ qubits, by applying the unitary $H^{\otimes n}$, followed by uniformly controlled R_z rotations with angles $\{\sqrt{\gamma}w_jx\}$, following the quantum amplitude encoding protocol of Ref. [44], in Fig. 2, we show a particular example for a 3 qubit circuit. To extend to higher dimensional data $\mathbf{x} \in \mathbb{R}^D$, we may prepare the objective state $|\psi(\mathbf{x})\rangle$ by composing the uniformly controlled R_z rotations, as illustrated in the j^{th} component $|\psi(\mathbf{x})\rangle^j = \sqrt{\frac{1}{d}} e^{i\sqrt{\gamma}\mathbf{w}_j \cdot \mathbf{x}} = \sqrt{\frac{1}{d}} \prod_k e^{i\sqrt{\gamma}w_{j,k}x_k}$, in this case, the composed uniformly controlled rotations have the form $R_z(\sqrt{\gamma}\mathbf{w}_j \cdot \mathbf{x}) = R_z(\sqrt{\gamma}w_{j,1}x_1)R_z(\sqrt{\gamma}w_{j,2}x_2) \dots R_z(\sqrt{\gamma}w_{j,D}x_D)$. In sum, the quantum variational circuit performs $(d-1)D$ rotations in the z axis with angles $\{\sqrt{\gamma}w_{j,k}x_k\}$. The preparation of these types of quantum variational states has been previously explored [18].

After the preparation of $|\psi(\mathbf{x})\rangle$ and $|\psi(\mathbf{y})\rangle$, we compute $\hat{k}_{\{\mathbf{w}_j\}}(\mathbf{x}, \mathbf{y}) = |\langle\psi(\mathbf{x})|\psi(\mathbf{y})\rangle|^2$, by the quantum kernel estimation protocol [43], see Fig. 2. Finally, to optimize the loss function, see Eq. 5, we initialize the variational parameters $\{w_{j,k}\}$ randomly between $[0, 1]$, and evaluate the derivatives using the classical Adam optimizer [46].

B. DMKDE quantum circuit with spectral decomposition

To implement the prediction phase of the DMKDE, see Eq. 3, we also propose a novel quantum protocol to estimate the expected value of a mixed state density matrix from its eigendecomposition in a qubit-based quantum computer, see Fig. 3. This circuit extends to qubits a

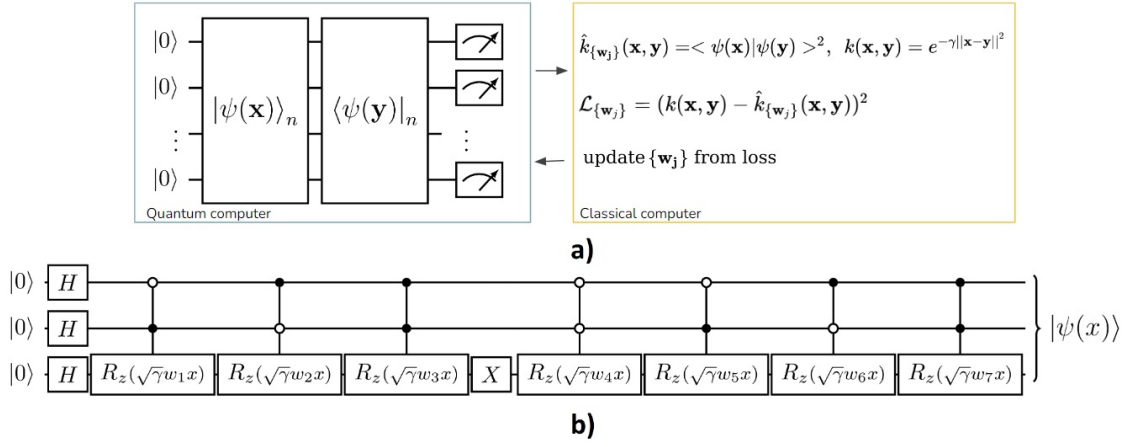


FIG. 2. **a)** Hybrid QAFF strategy with quantum kernel estimation protocol [43], **b)** Example of a quantum circuit to prepare the QAFF for one-dimensional data with 8 Fourier features and three qubits. This quantum state preparation follows Ref. [44].

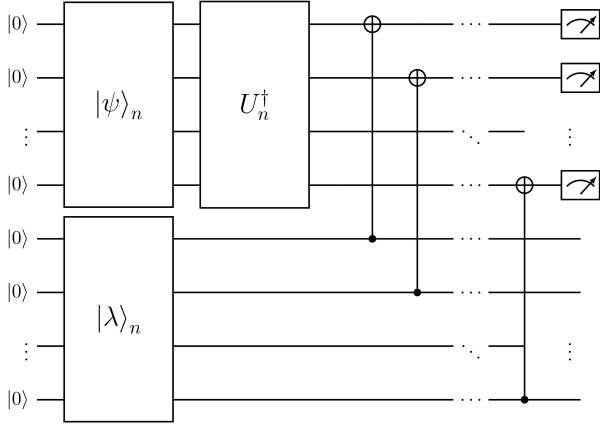


FIG. 3. DMKDE quantum circuit.

previous implementation of the mixed state DMKDE in a high-dimensional quantum computer [11].

We want to compute the expected value of a density matrix $\rho \in \mathbb{C}^{d \times d}$ with a quantum state $|\psi\rangle \in \mathbb{C}^d$ in a quantum computer. This calculation requires $2 \times n$ qubits, with $2^{n-1} < d \leq 2^n$. The first n qubits encode the state $|\psi\rangle$ and the unitary matrix V^\dagger whose rows are the complex conjugate eigenvectors of ρ , and the remaining n qubits encode the eigenvalues of the density matrix.

To begin with, as noted in [11], we have that,

$$\begin{aligned} \langle \psi | \rho | \psi \rangle &= \langle \psi | V \left(\sum_{i=0}^{d-1} \lambda_i |i\rangle \langle i| \right) V^\dagger | \psi \rangle \\ &= \sum_{i=0}^{d-1} \lambda_i |\langle i | V^\dagger | \psi \rangle|^2, \end{aligned} \quad (6)$$

where, $V \in \mathbb{C}^{d \times d}$ is the unitary matrix of eigenvectors and $\Lambda = \sum_{i=0}^{d-1} \lambda_i |i\rangle \langle i|$ is the diagonal matrix of eigenvalues.

The proposed DMKDE quantum circuit starts by ini-

tializing the first n qubits with the state $|\psi\rangle_n$, see the notation in Sect. III C, and the remaining n qubits with the state $|\lambda\rangle_n = \sum_{i=0}^{d-1} \sqrt{\lambda_i} |i\rangle_n$, state that encodes the eigenvalues of ρ , see Fig. 3. This operation can be performed thanks to amplitude encoding [44, 47]. We have that,

$$|\psi\rangle_n \otimes |\lambda\rangle_n = |\psi\rangle_n \otimes \sum_{i=0}^{d-1} \sqrt{\lambda_i} |i\rangle_n. \quad (7)$$

Next, we construct a unitary matrix U_n^\dagger , see Eq. 8, whose first quadrant is composed of the unitary matrix V^\dagger and its fourth quadrant with an identity matrix I with rank $2^n - d$,

$$U_n^\dagger = \left(\begin{array}{c|c} V^\dagger & \\ \hline & I \end{array} \right), \quad (8)$$

this unitary matrix U_n^\dagger is applied to the first n qubits in the form of an isometry [42]. We would have,

$$U_n^\dagger |\psi\rangle_n \otimes \sum_{i=0}^{d-1} \sqrt{\lambda_i} |i\rangle_n. \quad (9)$$

We can write the state of the first n qubits as, $U_n^\dagger |\psi\rangle_n = \sum_{i=0}^{d-1} a_i |i\rangle_n$. Where,

$$|a_i|^2 = |\langle i | U_n^\dagger | \psi \rangle|^2 = |\langle i | V^\dagger | \psi \rangle|^2, \quad (10)$$

namely, $|a_i|^2$ is the probability to measure $U_n^\dagger |\psi\rangle_n$ in the canonical state $|i\rangle_n$. Therefore, the circuit leads,

$$\begin{aligned} U_n^\dagger |\psi\rangle_n \otimes |\lambda\rangle_n &= \sum_{i=0}^{d-1} a_i |i\rangle_n \otimes \sum_{j=0}^{d-1} \sqrt{\lambda_j} |j\rangle_n \\ &= \sum_{i=0}^{d-1} a_i \sqrt{\lambda_i} |i\rangle_n \otimes |i\rangle_n + \sum_{\{(i,j):i \neq j\}} a_i \sqrt{\lambda_j} |i\rangle_n \otimes |j\rangle_n. \end{aligned}$$

We then apply a cascade of n CNOT gates, between the first and the second halves of the circuit, as shown in Fig. 3. The i^{th} CNOT operates with control the $(i+n)^{\text{th}}$ qubit and target the i^{th} qubit, with $i \in \{0, \dots, n-1\}$. The effect of this series of CNOT gates can be observed by writing,

$$|i\rangle_n \otimes |j\rangle_n = \left| \sum_{k=0}^{n-1} b_k^i 2^k \right\rangle_n \otimes \left| \sum_{l=0}^{n-1} b_l^j 2^l \right\rangle_n, \quad (11)$$

where, $|b_0^i b_1^i \dots b_{n-1}^i\rangle$ and $|b_0^j b_1^j \dots b_{n-1}^j\rangle$ are the binary representations of $|i\rangle_n$ and $|j\rangle_n$ respectively. The n CNOT gates have the same complexity as a single CNOT, as they can be parallelized in a quantum computer [48].

We represent this series of n CNOT gates with the $2n$ -qubit unitary operation U_{2n}^{Cn} , where Cn stands for CNOT. The outcome of this transformation is a qubit-wise summation modulo 2 (denoted by \oplus) on the first half of the circuit,

$$U_{2n}^{\text{Cn}}(|i\rangle_n \otimes |j\rangle_n) = \left| \sum_{k=0}^{n-1} (b_k^i \oplus b_k^j) 2^k \right\rangle_n \otimes \left| \sum_{l=0}^{n-1} b_l^j 2^l \right\rangle_n. \quad (12)$$

If $i = j$, we would have that,

$$U_{2n}^{\text{Cn}}(|i\rangle_n \otimes |i\rangle_n) = |0\rangle_n \otimes \left| \sum_{l=0}^{n-1} b_l^i 2^l \right\rangle_n \quad (13)$$

In contrast, if $i \neq j$, the state $\left| \sum_k (b_k^i \oplus b_k^j) 2^k \right\rangle_n$ would be distinct to the $|0\rangle_n$ state.

Therefore, after applying the series of n CNOT gates, the resulting state of the DMKDE quantum circuit is,

$$\begin{aligned} & \sum_{i=0}^{d-1} a_i \sqrt{\lambda_i} |0\rangle_n \otimes |i\rangle_n \\ & + \sum_{\{(i,j):i \neq j\}} a_i \sqrt{\lambda_j} \left| \sum_k (b_k^i \oplus b_k^j) 2^k \right\rangle_n \otimes |j\rangle_n. \end{aligned} \quad (14)$$

By measuring the first n qubits the probability of state $|0\rangle_n$ would be,

$$P(|0\rangle_n) = \sum_{i=0}^{d-1} |a_i|^2 \lambda_i = \sum_{i=0}^{d-1} \lambda_i |\langle i | V^\dagger | \psi \rangle|^2 = \langle \psi | \rho | \psi \rangle, \quad (15)$$

see Eqs. 6 and 10.

In contrast to the classical algorithm for expected value estimation with complexity $O(d^2)$, the proposed DMKDE quantum algorithm has complexity $O(2 \times \log d)$ measured by the number of qubits to encode the density matrix. In addition, the ansatz used for expected value estimation can be used to initialize a density matrix from its spectral decomposition starting from the $|0\rangle_{2n}$ state in a quantum computer, as illustrated in the SDM (spectral density matrix) ansatz in App. A.

C. Additional method: Non-orthogonal DMKDE for training in quantum hardware

The numeral (ii) of the classical-quantum density estimation method presents the training phase of the al-

gorithm in classical hardware, i.e, we build the training density matrix and perform its spectral decomposition in a classical computer. This approach is suitable for near-term quantum computers, since, we are allowed to codify the training density matrix based on its eigenvalues and eigenvectors with a low number of qubits ($2 \times \log d$ with d the dimension of the training density matrix), thanks to the DMKDE quantum algorithm, see Sect. IV B. However, the spectral decomposition of a large training density matrix in a classical computer has a large computational complexity of the order $O(d^3)$. For these scenarios, we propose to estimate the expected value of the training density matrix, see Eq. 3, with the non-orthogonal DM ansatz, see App. B; in this algorithm, we codify the training density matrix as a mixture of non-necessarily orthogonal pure states. This algorithm requires greater circuit depth, and $2 \times \log(\max(d, N))$ qubits, with N the number of training samples, therefore, we trade quantum computational complexity to avoid the spectral decomposition of the training density matrix in a classical computer.

D. Computational complexity analysis

To analyze the computational complexity of the proposed quantum density estimation algorithms, we assume N training data points and M testing samples whose density we aim to estimate, and we recall that QRFF and QAFF map D -dimensional classical data points to a d -dimensional quantum state.

DE Method	Train complexity	Test complexity
KDE [6, 7]	-	$O(DNM)$
C-DMKDE [14]	$O(d^2 N)$	$O(d^2 M)$
CQ-DMKDE	$O(d^2 \max(d, N))$	$O(dM)$
QNO-DMKDE	$O(dN)$	$O(dM)$

TABLE I. Comparison of the computational complexity of the classical and quantum density estimation methods in training and prediction phases, with N training data points, M test samples, D the dimension of the classical data, and d the dimension of the quantum feature map.

In Table I, we summarize the computational complexity of the training and prediction phase from top to bottom of the methods: kernel density estimation (KDE), DMKDE in classical hardware (C-DMKDE), the proposed classical-quantum implementation of the DMKDE (CQ-DMKDE), and the quantum non-orthogonal DMKDE (QNO-DMKDE). For the classical and quantum implementations of the DMKDE, we divide the complexity into training and testing stages, which means building the training density matrix in classical or quantum hardware for the training stage, see Eq. 2, and performing the density estimation of test samples, see Eq. 3, for the test step.

The KDE algorithm [6, 7] performs the training and prediction stages in a single computational step; for each

test sample, it involves computing the kernel with all the training data, hence the algorithm scales in the form $O(DNM)$. Aside from the complexity of the quantum Fourier feature map, the implementation of the DMKDE in a classical computer [14] requires building the training density matrix with complexity $O(d^2N)$, and computing the expectation value between each test quantum state and the training density matrix with complexity $O(d^2M)$. In addition, our proposed hybrid DMKDE builds the training density matrix in a classical computer, with complexity $O(d^2 \max(d, N))$, considering that it takes $O(d^2N)$ to build the density matrix, $O(d^3)$ to perform its spectral decomposition in a classical computer, and $O(d^2)$ and $O(d)$ to codify respectively the unitary and the eigenvalues of the density matrix in the quantum computer, also it performs the testing stage with complexity $O(dM)$ because it requires $O(dM)$ to read the testing data and codify the samples in the quantum computer with qRAM [49], and it takes $O(\log(d^2M))$ to measure the expected values of all testing data with the training density matrix, as explained in Sect. IV B. Furthermore, the non-orthogonal DMKDE has complexity $O(dN)$ to build the training density matrix in a quantum computer, see App. B, since it involves reading the training data and codifying the data in a quantum computer which has complexity $O(dN)$ (the same complexity of quantum state preparation), for the testing stage the quantum algorithm requires $O(dM)$ to read the test data and $O(\log(\max(d, N)^2M))$ to perform the density estimation, hence the complexity of the test step is $O(dM)$.

Overall, the KDE has the highest complexity out of all the methods, and both the CQ-DMKDE and the QNO-DMKDE reduce the complexity of the C-DMKDE, considering that these methods reduce the estimation of the expectation values to logarithmic complexity. Although the non-orthogonal DMKDE has the lowest complexity out of the four methods, the proposed classical-quantum DE method is suitable for NISQ computers because it is grounded in the DMKDE quantum algorithm which has a manageable number of qubits and a relatively-low circuit depth.

V. METHOD EVALUATION

In this section, we present the results of the proposed classical-quantum density estimation method for one and two-dimensional density estimation.

A. One-dimensional quantum density estimation

We present the experiments and results of one-dimensional density estimation in both a quantum simulator and a real quantum computer.

1. Experimental setup

As mentioned in Sect. IIIB, the DMKDE algorithm along with quantum random or adaptive Fourier features encodes in a density matrix a probability distribution of the training data and estimates the probability density of new testing samples by computing an expectation value.

To test the DMKDE quantum algorithm with the quantum adaptive Fourier features, we constructed a one-dimensional probability density distribution corresponding to a mixture of two Gaussians. The training data set was composed of 1000 points sampled from the pdf, whose probability density we aimed to estimate, and the testing data set was formed by 250 equidistant points in $[-7, 7]$.

Two quantum feature maps based on QAFF and QRFF were applied to both train and test data sets; we choose features of 4 components with $\gamma = 1$, for both adaptive and random features. We found that a value of γ with the same order of magnitude as the inverse of the variance of the training data was appropriate for density estimation. We used the QAFF variational algorithm to approximate a kernel for this data set; we used a set of 1-dimensional data points between $[-8, 8]$ to learn the appropriate weights of the adaptive Fourier features, using a noiseless simulator of the pennylane library [50], and used these weights to build the QAFF of the training and test data sets by making predictions on these two sets. As conventional RFF [16], the weights of the quantum random Fourier features were sampled from $\mathcal{N}(0, 1)$. For both quantum feature embeddings, we constructed training density matrices of dimensions 4×4 , see Eq. 2, and calculated their spectral decompositions, in a classical computer.

For the prediction step, we computed the probability density estimator, see Eq. 3, which corresponds to the expected value of the training density matrix, with our proposed DMKDE quantum circuit, see Fig. 3; we required 4 qubits to encode the 4×4 training density matrices and we executed 12000 shots in both the quantum simulator and the real quantum computer. Since we worked with a low number of features, we also performed a normalization of the density values by subtracting the minimum value from the density estimates.

2. Results and discussion

We report 3 experiments, see Fig. 4, two experiments with the noisy QASM simulator for the DMKDE and both QRFF and QAFF, and another experiment with QAFF and computing the density estimator with the real IBM-Oslo quantum computer.

In the subfigures of the left and center of Fig. 4, we show the probability density estimation with both quantum random and adaptive Fourier features with the QASM simulator. In comparison with QRFF, the QAFF creates a better approximation of the pdf, especially in

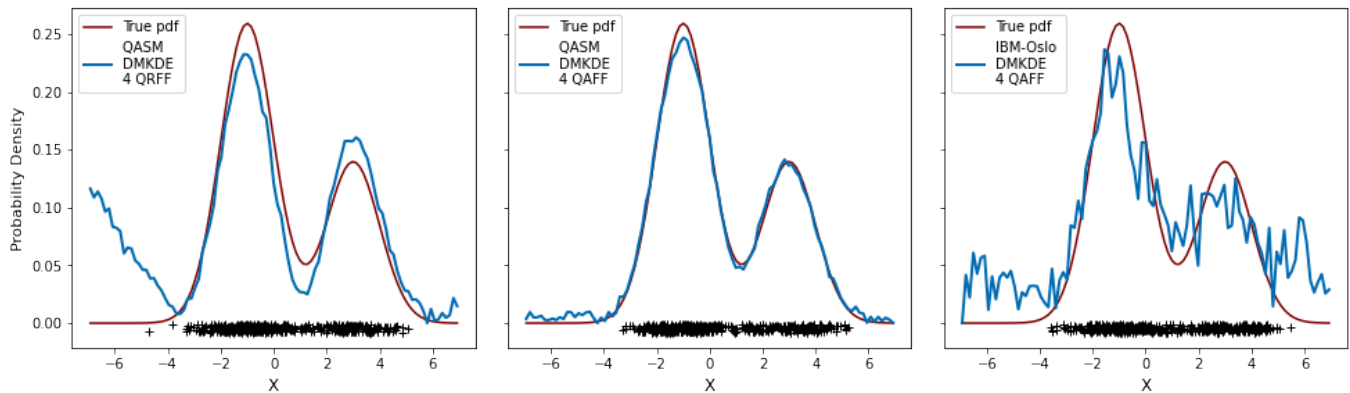


FIG. 4. Results of one-dimensional classical-quantum density estimation with 4 Fourier features: left, DE with QRFF in QASM simulator, center, DE with QAFF learned in pennylane simulator and predictions in QASM simulator, right, DE with QAFF learned in pennylane and DMKDE predictions in real IBM-Oslo quantum computer.

low-density regions. It should be highlighted that for QRFF, we chose the best-performing features for density estimation, out of 20 random Fourier configurations; in contrast, for QAFF, we obtained satisfactory density estimation results through multiple training iterations. In the subfigure of the right of Fig. 4, we present the results of QAFF learned with pennylane, and predicted with the DMKDE quantum algorithm, in the real IBM-Oslo quantum computer. As expected the results in the real quantum computer were much noisier than the results in the QASM simulator, however, the results show that it is possible to perform 1-Dimensional density estimation on noise-intermediate-scale quantum computers [20].

B. Two-dimensional quantum density estimation

We illustrate the proposed hybrid density estimation method for two-dimensional density estimation.

1. Experimental setup

We estimated the probability density functions of five two-dimensional data sets sampled from five two-dimensional distributions [45], called from top to bottom: 2D Mixture, Potential 1, Potential 2, Arc and Star Eight, see Fig. 5; the characteristics of these distributions are described in App. C. We performed the density estimations with three models: kernel density estimation (KDE), as a reference model, and the DMKDE with both QRFF and QAFF with 16 components. The training data set of the models corresponded to 10000 points sampled from the two-dimensional distributions, while the test data set was built by dividing the five two-dimensional spaces by grids of 120×120 points.

The results of the DMKDE with QAFF and QRFF were built using a noiseless simulator of the pennylane

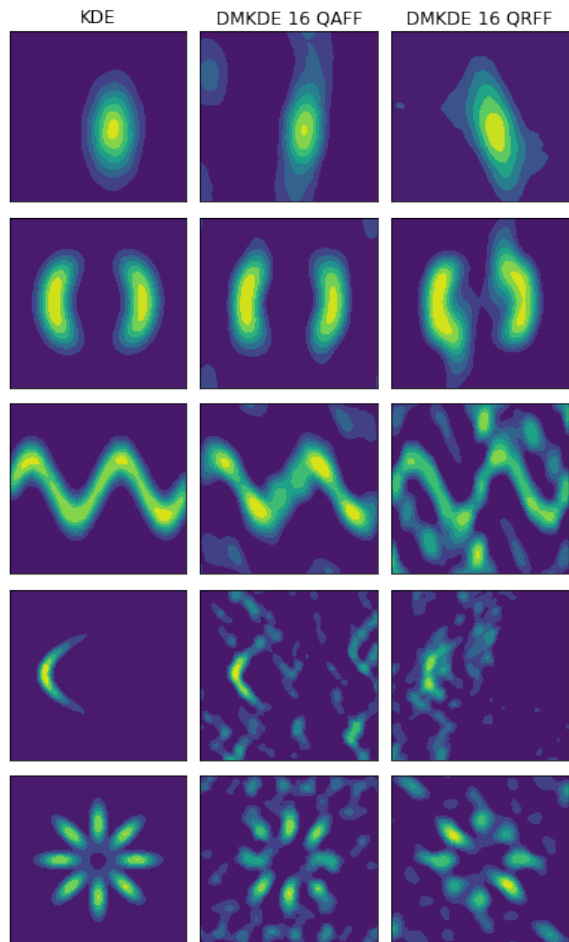


FIG. 5. Two-dimensional quantum density estimation with pennylane simulator. From top to bottom, the two-dimensional data sets correspond to 2D Mixture, Potential 1, Potential 2, Arc, and Star Eight.

library. To construct the quantum adaptive Fourier feature map, we used the QAFF strategy, as described in Sect. IV A. The QAFF variational method was built using 4 qubits, and $15 \times 2 = 30$ quantum variational parameters, which correspond to the angles of the QAFF ansatz. To learn the kernel of each two-dimensional data set, we looked for the optimal γ (gamma) parameter; as in the 1-dimensional case, the optimal γ had the same order of magnitude as the inverse of the variance of the training data. Furthermore, to train the QAFF, we used a kernel training data set composed of both the training data set and uniform points sampled in a greater area around the training data, these uniform points were added to the training data set to improve the kernel density estimation for cases where the pair-wise distance is high. After learning the QAFF, we made predictions on the training and test data sets to obtain the corresponding quantum maps of both train and test data. In addition, the quantum random Fourier features were built by sampling from $\mathcal{N}(0, 1)$, as is usual in RFF. For each of the five 2-dimensional datasets, we used the same γ parameter for the three methods.

After we established the QAFF and the QRFF maps for each 2-D data set, we built the 4×4 training density matrices and found their spectral decompositions in a classical computer. We then measured the expected value of the training density matrix with the quantum Fourier states of the test data set, using the 8-qubit DMKDE quantum algorithm with pennylane, obtaining the density estimation of the test data set.

2. Results and discussion

In Fig. 5, we show the density estimation of the test data set for all five 2-D data sets; in the column of the left, we show the density estimation using kernel density estimation (KDE) [6, 7], in the figure at the middle, we show the quantum density estimation using 16 quantum adaptive Fourier features, and in the figures at the right, we show the quantum density estimation using 16 quantum random Fourier features.

Since DMKDE with QAFF and QRFF are both approximations of KDE, we aimed to replicate the 2-dimensional density estimation results of the KDE in all data sets. As expected, the DMKDE with QAFF obtained better density estimation results in comparison with the random features, since the quantum adaptive Fourier features were optimized using the variational QAFF circuit. The results of the DMKDE with QRFF were also satisfactory given the low number of quantum components. Out of the five data sets, the Arc and Star Eight data sets were the most challenging for density estimation considering that these two data sets require a good approximation of the kernel for both low and high pairwise distances.

It is worth mentioning that the proposed hybrid density estimation method is non-parametric, i.e., it does not

require a prior probability distribution to fit the data, in contrast to parametric density estimation [21, 22], and is optimization-free. Furthermore, although we did not measure two-dimensional density estimation in real quantum hardware, the quantum simulation used a low number of qubits (8 qubits) which indicates that this hybrid method is suitable for NISQ devices.

VI. METHOD APPLICATION: QUANTUM ANOMALY DETECTION

In this section, we state a classical-quantum anomaly detection strategy as an application of our proposed hybrid density estimation method, see Fig. 6.

Anomaly detection (AD) aims to determine which samples from a given data set are “ordinary” or “normal” (being the interpretation of “normal” defined for each particular case) and which samples depart, or are deviated, from “normal” data (commonly known as “anomalies”). Some common applications of anomaly detection methods include fraud detection [51] and medical diagnosis [52]. This problem has been widely addressed in classical computers [53, 54], while quantum anomaly detection is a recent field, from which some proposals have shown notable speed-ups in contrast to their classical counterparts [10, 55, 56].

To detect anomalies in a particular dataset, the proposed method starts by dividing the data samples into three partitions: train, validation, and test expecting the same proportion of “normal” and “anomalous” data in all three partitions. After this, the method performs the following steps: i) use the proposed classical-quantum density estimation method to estimate the probability density values of all samples in validation and test partitions with the training partition, ii) use the validation data set to select a percentile-based threshold to separate the samples: if a sample has a density lower than the threshold, then it is considered an “anomalous” sample, and iii) finally, use this threshold to classify “normal” and “anomalous” data in the test partition. The main assumption in which we base this technique is that in contrast to “normal” samples, the “anomalous” samples lie in regions with lower probability density values, as shown in Fig. 6.

A. QAD: Experimental setup

We used the hybrid density estimation method to perform anomaly detection in a previously labeled AD dataset. For this purpose, we used a modified version, from Ref. [57], of the Cardiotocography dataset from the UCI Machine Learning Repository, related to fetal heart rate. It consists of 1831 samples, where each sample contains 21 attributes, with two classes: the *normal* class for the inliers, and the *pathologic* class for the outliers. This dataset was divided into three partitions: train (60%),

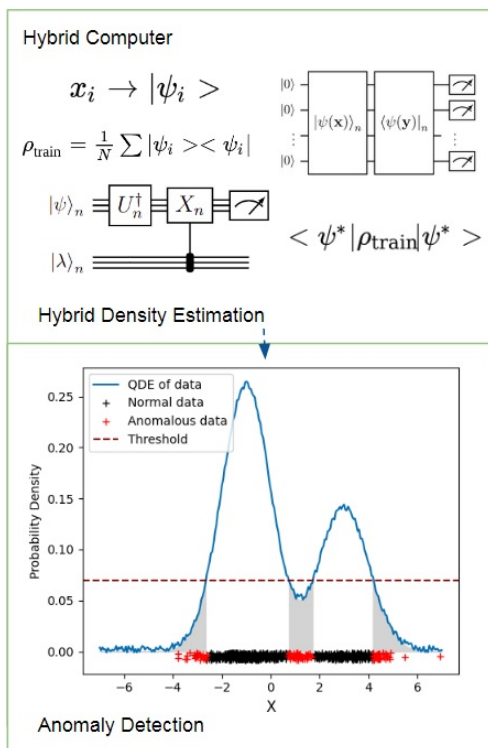


FIG. 6. Classical-quantum anomaly detection model for NISQ computers based on the proposed hybrid density estimation strategy.

validation (20%), and test (20%), all of which contained both normal samples and outliers in the same proportion (approximately, 9.6% of all samples were labeled as outliers).

As a first step, QRFF and QAFF were applied to the samples of all partitions as quantum feature mappings. We worked with 4 Fourier features which corresponded to quantum states of 2 qubits. The QAFF were obtained with the QAFF variational method with a noiseless simulator of the pennylane library, we used the training data to learn the kernel of the adaptive features, this quantum variational circuit required 21×3 variational parameters. We searched for the optimal values of γ of the kernel (considering only powers of two ranging from 2^{-10} to 2^0), for the experiments in the quantum simulator we set $\gamma = 2^{-7}$, whereas, a value of $\gamma = 2^{-5}$ for the real quantum computer.

We then used a classical computer to build the 4×4 training density matrices, see Eq. 2, and to compute their spectral decompositions. We then performed the density estimations with the DMKDE quantum algorithm in the pennylane simulator and the real IBM-Oslo quantum computer. As usual in anomaly detection algorithms, labels were not used during the training phase.

After performing the density estimations of the validation and test partitions, we classified each sample as “normal” or “outlier” by comparing its density value with a threshold value t . We used the validation partition to

search for the threshold by setting a percentile value p such that 9.6% of samples had a density below t , thus being considered as anomalies. We then used the obtained boundary t to classify the testing samples.

We report the accuracy, AUC (area under the characteristic curve), and F1 Score of the “anomalous” class. Considering that the experiments depend on the initial random parameters, for each quantum mapping, we did ten experiments in the quantum simulator, while executing only one experiment in the real quantum computer.

B. QAD: Results and discussion

The results of the proposed hybrid anomaly detection method in the quantum simulator are presented in Table II. In comparison with QRFF, the QAFF obtained better results in the three evaluated metrics, F1 Score, accuracy, and AUC, thanks to the optimization of the Fourier weights. Regarding the standard deviations, we observe more consistent results across different experiments with QAFF, which shows that QRFF is more sensitive to randomness than QAFF in a low-dimensional setting.

Feature Map	F1 Score	Accuracy	AUC
QRFF: 4	0.422 ± 0.073	0.896 ± 0.013	0.776 ± 0.061
QAFF: 4	0.660 ± 0.017	0.936 ± 0.003	0.952 ± 0.005

TABLE II. Obtained metrics for 10 hybrid anomaly detection experiments on Cardio dataset using DMKDE with 4 Fourier features for both QRFF and QAFF with pennylane quantum simulator.

Furthermore, in Table III, we present the results of the hybrid anomaly detection algorithm in the real IBM-Oslo quantum computer; only one experiment is reported for each quantum mapping. The results follow a similar pattern as the quantum simulator: QAFF leads to higher performance in comparison to QRFF. In contrast to the quantum simulator, the experiment with QRFF in the real quantum computer presented inferior results, probably because the density values with random features were highly concentrated on a particular value, therefore, the quantum noise was detrimental to differentiate the two classes. Nonetheless, the DMKDE with QAFF in the real quantum computer obtained satisfactory results for the anomaly detection task, hence the proposed hybrid DE strategy is suitable for near-term quantum devices.

VII. CONCLUSIONS

In this article, we presented a classical-quantum density estimation method for current noisy quantum computers. The method is grounded on a proposed quantum implementation of the DMKDE algorithm [14], and the new quantum variational data embedding called quantum adaptive Fourier features. Within our DE method,

Feature Map	F1 Score	Accuracy	AUC
QRFF: 4	0.170	0.867	0.541
QAFF: 4	0.648	0.932	0.933

TABLE III. Obtained metrics for the hybrid anomaly detection experiments using a real IBM quantum computer (IBM-Oslo) using DMKDE with both QRFF and QAFF with 4 Fourier components. We used the pennylane quantum simulator to learn the optimal QAFF, and the real quantum computer to predict the density of validation and test samples with the DMKDE quantum circuit.

we presented two quantum algorithms to estimate the expected value of a density matrix from its eigendecomposition, and as a mixture of non-orthogonal pure states, the protocols allow to encode density matrices in quantum computers with a logarithmic number of qubits. Furthermore, we introduced the QAFF, a new quantum variational strategy for kernel learning, which learns in quantum hardware the optimal weights of random Fourier features [16].

We illustrated the hybrid DE method for one and two dimensional density estimation in a quantum simulator and a real quantum computer, and with two quantum embeddings: quantum random and adaptive Fourier features. The DE results show that it is possible to exploit the characteristics of mixed states and Fourier features to efficiently represent probability distributions of data in quantum hardware. Furthermore, we highlight that the proposed hybrid DE strategy is optimization-free, namely, besides the quantum mapping the method does not require optimization, and it is non-parametric, i.e., it does not assume a prior probability distribution to fit the training data, in contrast to, parametric quantum DE methods based on multivariate Gaussian distributions [10, 13]. In comparison to QRFF, the experimental results in the quantum simulator and the real quantum computer showed that the combination of the DMKDE quantum algorithm with QAFF allows to perform one

and two dimensional density estimation with a low number of Fourier features, and accordingly with relatively-small quantum circuits. Hence, the proposed hybrid DE strategy is suitable for NISQ computers [20].

We also presented an application of the quantum density estimation method for anomaly detection in a quantum simulator and a real quantum computer. Despite the current limitations of quantum hardware, the DMKDE with QAFF showed satisfactory results for anomaly detection in both the simulator and the real quantum computer. In addition, considering the numerous applications of density estimation [1–5], the experimental results illustrate that the proposed hybrid density estimation method can be used as a building block for other quantum machine learning algorithms on NISQ computers [20].

Future work of the proposed classical-quantum DE technique includes comparing the performance of our method with other classical and quantum density estimation methods and also increasing the number of Fourier features, hence augmenting the size of the quantum circuits (given the near-term limitations in quantum hardware). Besides, we aim to apply quantum adaptive Fourier features as mapping functions to other kernel methods and to study their theoretical implications and performance. An interesting future endeavor involves integrating the proposed DMKDE quantum circuit with variational quantum algorithms to learn mixed quantum states in a quantum computer.

ACKNOWLEDGMENTS

We acknowledge the use of IBM Quantum services for this work. The views expressed in this work are those of the authors and do not reflect the official policy or position of IBM or the IBM Quantum team.

-
- [1] C. Fraley and A. E. Raftery, Model-based clustering, discriminant analysis, and density estimation, *Journal of the American statistical Association* **97**, 611 (2002).
 - [2] T. K. Anderson, Kernel density estimation and k-means clustering to profile road accident hotspots, *Accident Analysis & Prevention* **41**, 359 (2009).
 - [3] B. Nachman and D. Shih, Anomaly detection with density estimation, *Phys. Rev. D* **101**, 075042 (2020).
 - [4] W. Hu, J. Gao, B. Li, O. Wu, J. Du, and S. Maybank, Anomaly detection using local kernel density estimation and context-based regression, *IEEE Transactions on Knowledge and Data Engineering* **32**, 218 (2018).
 - [5] S. A. Bigdeli, G. Lin, T. Portenier, L. A. Dunbar, and M. Zwicker, Learning generative models using denoising density estimators, arXiv preprint arXiv:2001.02728 (2020).
 - [6] M. Rosenblatt, Remarks on Some Nonparametric Estimates of a Density Function, <https://doi.org/10.1214/aoms/1177728190> **27**, 832 (1956).
 - [7] E. Parzen, On Estimation of a Probability Density Function and Mode, *The Annals of Mathematical Statistics* **33**, 1065 (1962).
 - [8] Z. Wang and D. W. Scott, Nonparametric density estimation for high-dimensional data—algorithms and applications, *Wiley Interdisciplinary Reviews: Computational Statistics* **11**, e1461 (2019).
 - [9] G. Papamakarios, T. Pavlakou, and I. Murray, Masked autoregressive flow for density estimation, *Advances in neural information processing systems* **30** (2017).
 - [10] J.-M. Liang, S.-Q. Shen, M. Li, and L. Li, Quantum anomaly detection with density estimation and multivariate gaussian distribution, *Physical Review A* **99**, 052310

- (2019).
- [11] D. H. Useche, A. Giraldo-Carvajal, H. M. Zuluaga-Bucheli, J. A. Jaramillo-Villegas, and F. A. González, Quantum measurement classification with qudits, *Quantum Information Processing* 2021 21:1 **21**, 1 (2021).
- [12] V. Vargas-Calderón, F. A. González, and H. Vinck-Posada, Optimisation-free density estimation and classification with quantum circuits, *Quantum Machine Intelligence* **4**, 1 (2022).
- [13] M. Guo, H. Liu, Y. Li, W. Li, F. Gao, S. Qin, and Q. Wen, Quantum algorithms for anomaly detection using amplitude estimation, *Physica A: Statistical Mechanics and its Applications* **604**, 127936 (2022).
- [14] F. A. González, A. Gallego, S. Toledo-Cortés, and V. Vargas-Calderón, Learning with density matrices and random features, *Quantum Machine Intelligence* **4**, 1 (2022).
- [15] J. A. Gallego, J. F. Osorio, and F. A. Gonzalez, Fast kernel density estimation with density matrices and random fourier features, in *Ibero-American Conference on Artificial Intelligence* (Springer, 2022) pp. 160–172.
- [16] A. Rahimi and B. Recht, Random features for large-scale kernel machines, in *Advances in Neural Information Processing Systems 20 - Proceedings of the 2007 Conference* (2009).
- [17] D. F. James, P. G. Kwiat, W. J. Munro, and A. G. White, Measurement of qubits, *Physical Review A* **64**, 052312 (2001).
- [18] M. Schuld, R. Sweke, and J. J. Meyer, Effect of data encoding on the expressive power of variational quantum-machine-learning models, *Physical Review A* **103**, 032430 (2021).
- [19] Y. Li, K. Zhang, J. Wang, and S. Kumar, Learning adaptive random features, in *Proceedings of the AAAI Conference on Artificial Intelligence*, Vol. 33 (2019) pp. 4229–4236.
- [20] J. Preskill, Quantum computing in the nisq era and beyond, *Quantum* **2**, 79 (2018).
- [21] M. K. Varanasi and B. Aazhang, Parametric generalized gaussian density estimation, *The Journal of the Acoustical Society of America* **86**, 1404 (1989).
- [22] V. Vapnik and S. Mukherjee, Support vector method for multivariate density estimation, *Advances in neural information processing systems* **12** (1999).
- [23] P. Rebentrost, M. Mohseni, and S. Lloyd, Quantum support vector machine for big data classification, *Physical review letters* **113**, 130503 (2014).
- [24] C. Blank, A. J. da Silva, L. P. de Albuquerque, F. Petrucione, and D. K. Park, Compact quantum distance-based binary classifier, *arXiv preprint arXiv:2202.02151* (2022).
- [25] C. Blank, D. K. Park, J.-K. K. Rhee, and F. Petrucione, Quantum classifier with tailored quantum kernel, *npj Quantum Information* **6**, 1 (2020).
- [26] G. Sergioli, R. Giuntini, and H. Freytes, A new quantum approach to binary classification, *PloS one* **14**, e0216224 (2019).
- [27] N. A. Nghiem, S. Y.-C. Chen, and T.-C. Wei, Unified framework for quantum classification, *Physical Review Research* **3**, 033056 (2021).
- [28] C. H. Bennett, G. Brassard, S. Popescu, B. Schumacher, J. A. Smolin, and W. K. Wootters, Purification of noisy entanglement and faithful teleportation via noisy channels, *Physical review letters* **76**, 722 (1996).
- [29] A. Peruzzo, J. McClean, P. Shadbolt, M.-H. Yung, X.-Q. Zhou, P. J. Love, A. Aspuru-Guzik, and J. L. O’Brien, A variational eigenvalue solver on a photonic quantum processor, *Nature communications* **5**, 1 (2014).
- [30] M. A. Nielsen and I. L. Chuang, *Quantum Computation and Quantum Information: 10th Anniversary Edition*, *Quantum Computation and Quantum Information* 10.1017/CBO9780511976667 (2010).
- [31] M. Cramer, M. B. Plenio, S. T. Flammia, R. Somma, D. Gross, S. D. Bartlett, O. Landon-Cardinal, D. Poulin, and Y. K. Liu, Efficient quantum state tomography, *Nature Communications* 2010 1:1 **1**, 1 (2010).
- [32] D. F. James, P. G. Kwiat, W. J. Munro, and A. G. White, On the measurement of qubits, *Asymptotic Theory of Quantum Statistical Inference: Selected Papers* , 509 (2005).
- [33] S. Lloyd, M. Mohseni, and P. Rebentrost, Quantum principal component analysis, *Nature Physics* **10**, 631 (2014).
- [34] F. A. González, V. Vargas-Calderón, and H. Vinck-Posada, Classification with quantum measurements, *Journal of the Physical Society of Japan* **90**, 044002 (2021), <https://doi.org/10.7566/JPSJ.90.044002>.
- [35] A. Kammonen, J. Kiessling, P. Plecháč, M. Sandberg, and A. Szepessy, Adaptive random fourier features with metropolis sampling, *Foundations of Data Science* **2**, 309 (2020).
- [36] Y. Liu, Y. Xu, J. Yang, and S. Jiang, A Polarized Random Fourier Feature Kernel Least-Mean-Square Algorithm, *IEEE Access* **7**, 50833 (2019).
- [37] R. Agrawal, T. Campbell, J. Huggins, and T. Broderick, Data-dependent compression of random features for large-scale kernel approximation, *AISTATS 2019 - 22nd International Conference on Artificial Intelligence and Statistics* 10.48550/arxiv.1810.04249 (2018).
- [38] J. Xie, F. Liu, K. Wang, and X. Huang, Deep kernel learning via random fourier features, *arXiv preprint arXiv:1910.02660* (2019).
- [39] E. G. Băzăvan, F. Li, and C. Sminchisescu, Fourier Kernel Learning, *Lecture Notes in Computer Science (including subseries Lecture Notes in Artificial Intelligence and Lecture Notes in Bioinformatics)* **7573 LNCS**, 459 (2012).
- [40] V. Havlíček, A. D. Córcoles, K. Temme, A. W. Harrow, A. Kandala, J. M. Chow, and J. M. Gambetta, Supervised learning with quantum-enhanced feature spaces, *Nature* **567**, 209 (2019).
- [41] R. Chatterjee and T. Yu, Generalized coherent states, reproducing kernels, and quantum support vector machines, *arXiv preprint arXiv:1612.03713* (2016).
- [42] R. Iten, R. Colbeck, I. Kukuljan, J. Home, and M. Christandl, Quantum circuits for isometries, *Phys. Rev. A* **93**, 032318 (2016).
- [43] Y. Liu, S. Arunachalam, and K. Temme, A rigorous and robust quantum speed-up in supervised machine learning, *Nature Physics* **17**, 1013 (2021).
- [44] V. V. Shende, S. S. Bullock, and I. L. Markov, Synthesis of quantum-logic circuits, *IEEE Transactions on Computer-Aided Design of Integrated Circuits and Systems* **25**, 1000 (2006).
- [45] J. A. Gallego and F. A. González, Quantum adaptive fourier features for neural density estimation (2022).
- [46] D. P. Kingma and J. Ba, Adam: A method for stochastic optimization, *arXiv preprint arXiv:1412.6980* (2014).

- [47] M. Möttönen, J. J. Vartiainen, V. Bergholm, and M. M. Salomaa, Transformation of quantum states using uniformly controlled rotations, *Quantum Information & Computation* **5**, 467 (2005).
- [48] L. Cincio, Y. Subaşı, A. T. Sornborger, and P. J. Coles, Learning the quantum algorithm for state overlap, *New Journal of Physics* **20**, 113022 (2018).
- [49] V. Giovannetti, S. Lloyd, and L. Maccone, Quantum random access memory, *Physical review letters* **100**, 160501 (2008).
- [50] V. Bergholm, J. Izaac, M. Schuld, C. Gogolin, M. S. Alam, S. Ahmed, J. M. Arrazola, C. Blank, A. Delgado, S. Jahangiri, *et al.*, Pennylane: Automatic differentiation of hybrid quantum-classical computations, arXiv preprint arXiv:1811.04968 (2018).
- [51] V. Van Vlasselaer, C. Bravo, O. Caelen, T. Eliassi-Rad, L. Akoglu, M. Snoeck, and B. Baesens, APATE: A novel approach for automated credit card transaction fraud detection using network-based extensions, *Decision Support Systems* **75**, 38 (2015).
- [52] L. F. Chen, An improved negative selection approach for anomaly detection: with applications in medical diagnosis and quality inspection, *Neural Computing and Applications* 2011 22:5 **22**, 901 (2011).
- [53] C. C. Noble and D. J. Cook, Graph-based anomaly detection, in *Proceedings of the ninth ACM SIGKDD international conference on Knowledge discovery and data mining* (2003) pp. 631–636.
- [54] F. A. González and D. Dasgupta, Anomaly detection using real-valued negative selection, *Genetic Programming and Evolvable Machines* **4**, 383 (2003).
- [55] N. Liu and P. Rebentrost, Quantum machine learning for quantum anomaly detection, *Physical Review A* **97**, 042315 (2018).
- [56] D. Herr, B. Obert, and M. Rosenkranz, Anomaly detection with variational quantum generative adversarial networks, *Quantum Science and Technology* **6**, 045004 (2021).
- [57] C. C. Aggarwal and S. Sathe, Theoretical Foundations and Algorithms for Outlier Ensembles, *ACM SIGKDD Explorations Newsletter* **17**, 24 (2015).
- [58] N. Ezzell, E. M. Ball, A. U. Siddiqui, M. M. Wilde, A. T. Sornborger, P. J. Coles, and Z. Holmes, Quantum mixed state compiling, arXiv preprint arXiv:2209.00528 (2022).
- [59] M. Möttönen, J. J. Vartiainen, V. Bergholm, and M. M. Salomaa, Quantum circuits for general multiqubit gates, *Physical review letters* **93**, 130502 (2004).

Appendix A: SDM ansatz, density matrix preparation from eigenbasis

The SDM (spectral density matrix) ansatz to initialize a density matrix $\rho \in \mathbb{C}^{d \times d}$ departing from its spectral decomposition requires $2 \times n$ qubits, such that $2^{n-1} < d \leq 2^n$. Let $\rho = U\Lambda U^\dagger$ be the spectral decomposition of the density matrix, where U is the matrix of eigenvectors and $\Lambda = \sum \lambda_i |i\rangle \langle i|$ is the diagonal matrix of eigenvalues. The protocol begins by initializing the first n qubits with the state $|\lambda\rangle_n = \sum_{i=0}^{d-1} \sqrt{\lambda_i} |i\rangle_n$, thanks to amplitude encoding [44, 47]. Therefore, the circuit starts with the state,

$$\sum_{i=0}^{d-1} \sqrt{\lambda_i} |\sum_k b_k^i 2^k\rangle_n \otimes |0\rangle_n, \quad (\text{A1})$$

where $|b_0^i b_1^i \dots b_{n-1}^i\rangle$ is the binary representation of the canonical state $|i\rangle_n$. Then, a cascade of n CNOT gates between the first and the second parts of the circuit is applied, as shown in Fig. 7. The j^{th} CNOT operates with control the j^{th} qubit and target the $(n+j)^{\text{th}}$ qubit for $j \in \{0, \dots, n-1\}$. The resulting quantum state of this operation is,

$$\sum_{i=0}^{d-1} \sqrt{\lambda_i} |\sum_k b_k^i 2^k\rangle_n \otimes |\sum_k b_k^i 2^k\rangle_n = \sum_{i=0}^{d-1} \sqrt{\lambda_i} |i\rangle_n \otimes |i\rangle_n. \quad (\text{A2})$$

It follows to perform a measurement on the purification [28] by measuring the last n qubits, which results in a mixed state in the first n qubits with only classical probability,

$$\Lambda_n = \sum_{i=0}^{d-1} \lambda_i |i\rangle \langle i|_n. \quad (\text{A3})$$

The desired density matrix is obtained by applying to the state Λ_n , an isometry [42], U_n , given by,

$$U_n = \left(\begin{array}{c|c} U & \\ \hline & I \end{array} \right), \quad (\text{A4})$$

where I has rank $2^n - d$, the process results in the desired mixed state,

$$\rho_n = U_n \Lambda_n U_n^\dagger. \quad (\text{A5})$$

as shown in Fig 7.

It should be highlighted that measuring the last n qubits after applying the isometry U_n leads to the same result. After the initial version of this manuscript, we became aware of a similar work [58] on mixed state preparation.

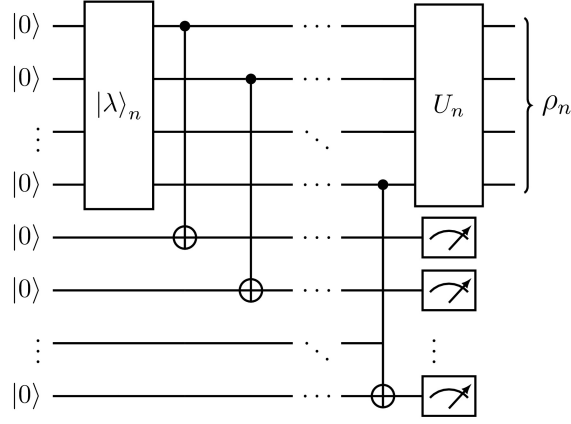


FIG. 7. SDM ansatz: mixed state initialization in the eigenbasis.

Appendix B: Non-orthogonal DM ansatz, mixture of non-orthogonal pure states

In general, a density matrix is presented as a statistical mixture of non-orthogonal pure states. Finding the spectral decomposition of a density matrix has large computational complexity in classical computers. Hence, we present a novel quantum protocol to initialize and estimate the expected value of a density matrix which is presented as a mixture of non-orthogonal pure states. We wish to initialize a density matrix $\rho = \sum_{i=0}^{N-1} p_i |\psi_i\rangle \langle \psi_i|$, with p_i the classical probabilities, and $|\psi_i\rangle \in \mathbb{C}^d$ the pure states that form the ensemble. To create the mixed state ρ , we require $2 \times m$ qubits, where $2^{m-1} < \max(N, d) \leq 2^m$.

The method starts by initializing the pure state $|\xi\rangle_m = \sum_{i=0}^{N-1} \sqrt{p_i} |i\rangle_m$, on the first m qubits, followed by a cascade of m CNOT gates between the two halves of the circuit to form the entangled state $\sum_{i=0}^{N-1} \sqrt{p_i} |i\rangle_m \otimes |i\rangle_m$, see Fig. 8. It follows a series of N uniformly controlled isometries, with controls the last m qubits and targets the first m qubits; these controlled isometries are applied following the structure of a multiplexer gate [44, 59]. The i^{th} controlled isometry works by setting $|i\rangle_m$ as the controlled state from the second half of the circuit, and target the first m qubits, with the isometry U_m^i , such that $U_m^i |i\rangle_m \rightarrow |\psi_i\rangle_m$, as shown in Fig. 8. The resulting state of the transformation is the purification,

$$\sum_{i=0}^{N-1} \sqrt{p_i} |\psi_i\rangle_m \otimes |i\rangle_m. \quad (\text{B1})$$

To build the desired mixed state, we perform a partial trace by measuring all the m qubits of the second half of the circuit, obtaining the state,

$$\rho_m = \sum_{i=0}^{N-1} p_i |\psi_i\rangle \langle \psi_i|_m, \quad (\text{B2})$$

on the first m qubits.

To implement the non-orthogonal DMKDE, we do not measure the last m qubits, instead, starting from the purification, see Eq. B1, with $|\xi\rangle_m = \sum_{i=0}^{N-1} \sqrt{1/N} |i\rangle_m$ and $\{|\psi_i\rangle\}$ the training quantum states, we apply an isometry U_m^\dagger to the first m qubits, that satisfies $U_m |0\rangle_m = |\psi\rangle_m$, with $|\psi\rangle$ the test quantum state, and then we measure these first m qubits, to obtain that $P(|0\rangle_m) = \langle \psi | \rho_{\text{train}} | \psi \rangle$. This quantum expected value proposal has complexity $O(\log(\max(N, d)))$ measured from the number of qubits required to build the density matrix.

Appendix C: Two Dimensional Datasets

We used five synthetic two-dimensional data sets from Ref. [45] to evaluate our proposed quantum density estimation method. The data sets are characterized as follows:

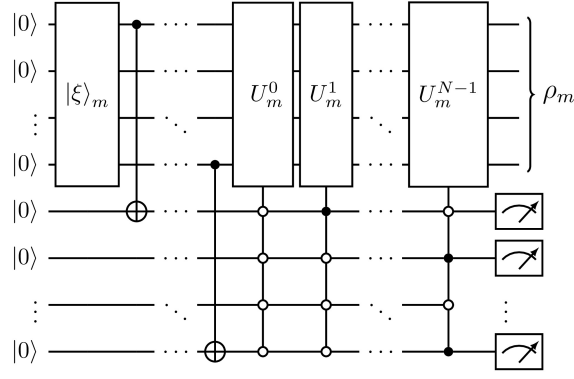


FIG. 8. Non-orthogonal DM ansatz: mixed state initialization with an ensemble of non-orthogonal pure states with uniformly controlled isometries.

- *2D mixture* dataset corresponds to a two-dimensional random sample drawn from the random vector $\mathbf{X} = (X_1, X_2)$ with a probability density function given by

$$f(\mathbf{x}) = \frac{1}{2}\mathcal{N}(\mathbf{x}|\boldsymbol{\mu}_1, \boldsymbol{\Sigma}_1) + \frac{1}{2}\mathcal{N}(\mathbf{x}|\boldsymbol{\mu}_2, \boldsymbol{\Sigma}_2)$$

with means and covariance matrices $\boldsymbol{\mu}_1 = [1, -1]^T$, $\boldsymbol{\mu}_2 = [-2, 2]^T$, $\boldsymbol{\Sigma}_1 = \begin{bmatrix} 1 & 0 \\ 0 & 2 \end{bmatrix}$, and $\boldsymbol{\Sigma}_2 = \begin{bmatrix} 2 & 0 \\ 0 & 1 \end{bmatrix}$

- *Potential 1* dataset corresponds to a two-dimensional random sample drawn from a random vector $\mathbf{X} = (X_1, X_2)$ with probability density function given by

$$f(\mathbf{x}_1, \mathbf{x}_2) = \frac{1}{2} \left(\frac{\|\mathbf{x}\| - 2}{0.4} \right)^2 - \ln \left(\exp \left\{ -\frac{1}{2} \left[\frac{\mathbf{x}_1 - 2}{0.6} \right]^2 \right\} + \exp \left\{ -\frac{1}{2} \left[\frac{\mathbf{x}_2 + 2}{0.6} \right]^2 \right\} \right)$$

with a normalizing constant of approximately 6.52 calculated by Monte Carlo integration.

- *Potential 2* dataset corresponds to a two-dimensional random sample drawn from a random vector $\mathbf{X} = (X_1, X_2)$ with probability density function given by

$$f(\mathbf{x}_1, \mathbf{x}_2) = \frac{1}{2} \left[\frac{\mathbf{x}_2 - w_1(\mathbf{x})}{0.4} \right]^2$$

where $w_1(\mathbf{x}) = \sin\left(\frac{2\pi x_1}{4}\right)$ with a normalizing constant of approximately 8 calculated by Monte Carlo integration.

- *Arc* dataset corresponds to a two-dimensional random sample drawn from a random vector $\mathbf{X} = (X_1, X_2)$ with probability density function given by

$$f(\mathbf{x}_1, \mathbf{x}_2) = \mathcal{N}(\mathbf{x}_2|0, 4)\mathcal{N}(\mathbf{x}_1|0.25\mathbf{x}_2^2, 1)$$

where $\mathcal{N}(u|\mu, \sigma^2)$ denotes the density function of a normal distribution with mean μ and variance σ^2 .

- *Star Eight* dataset corresponds to a two-dimensional random sample drawn from a random vector $\mathbf{X} = (X_1, X_2)$. The bivariate probability distribution function is generated from a Gaussian bivariate random variable \mathbf{z} as

$$f(\mathbf{x}_1, \mathbf{x}_2) = -\ln \left(e^{-\frac{1}{2} \left[\frac{\mathbf{z}_2 - w_1(\mathbf{z})}{0.35} \right]^2} + e^{-\frac{1}{2} \left[\frac{\mathbf{z}_2 - w_1(\mathbf{z}) + w_2(\mathbf{z})}{0.35} \right]^2} \right)$$

where $w_1(\mathbf{z}) = \sin\left(\frac{2\pi \mathbf{z}}{4}\right)$ and $w_2(\mathbf{z}) = 3e^{-\frac{1}{2} \left[\frac{\mathbf{z} - 1}{0.6} \right]^2}$.